Available online at www.sciencedirect.com
ScienceDirect
Proceedings of the Combustion Institute 000 (2018) 1–9
Proceedings of the Combustion Institute
www.elsevier.com/locate/proci

Alkali metal emissions in an early-stage pulverized-coal flame: DNS analysis of reacting layers and chemistry tabulation

Kaidi Wan [a], Luc Vervisch [b], Jun Xia [c,*], Pascale Domingo [b], Zhihua Wang [a,*], Yingzu Liu [a,c], Kefa Cen [a]

[a] State Key Laboratory of Clean Energy Utilization, Zhejiang University, Hangzhou 310027, China
[b] CORIA – CNRS, Normandie Université, INSA de Rouen, Saint-Etienne-du-Rouvray 76800, France
[c] Department of Mechanical and Aerospace Engineering & Institute of Energy Futures, Brunel University London, Uxbridge UB8 3PH, UK

Received 27 November 2017; accepted 15 June 2018
Available online xxx

Abstract

The intricate coupling between coal pyrolysis, gas phase combustion and the emissions of alkali metal, such as sodium, is studied in the early stage of a temporally evolving three-dimensional planar turbulent jet carrying pulverized-coal particles. Complex chemistry is used to account for both the combustion of volatile hydrocarbons and the sodium containing species. The response of the sodium chemistry is analyzed in the mixture fraction space, along with the topology of the reactions zones. Combustion is found to start preferentially in partially premixed flames, which then evolve toward diffusion-like reactive layers and reach chemical equilibrium. From the direct numerical simulation (DNS) database, the possibility of modeling the dynamics of sodium species using one-dimensional premixed flamelet generated manifolds (FGM) is investigated. A chemical lookup table is constructed for the combustion of the partially premixed volatiles and an additional three-dimensional simulation is performed to compare the tabulated sodium species against their reference counterparts with complex chemistry. Quantitative analysis of the performance of the developed chemistry tabulation confirms the validity of the approach. Perspectives for the modeling of sodium emissions in pulverized-coal furnaces and boilers are finally drawn.

Keywords: Pulverized-coal combustion; Direct numerical simulation; Sodium chemistry; Alkali metal; Chemistry tabulation

1. Introduction

Solid fuels, such as coal and biomass, are widely utilized to support the worldwide energy consumption due to their broad availability and the

* Corresponding authors.
E-mail addresses: jun.xia@brunel.ac.uk (J. Xia), wangzh@zju.edu.cn (Z. Wang).

https://doi.org/10.1016/j.proci.2018.06.119

overall flexibility of solid fuel combustion systems [1]. In practice, the presence of alkali metals such as sodium (Na) in coal and potassium (K) in biomass leads to massive ash depositions and corrosions in the solid-fuel-fired boilers [2]. These alkali-induced issues severely limit the utilization of coal and biomass with a relatively high concentration of alkali, such as Zhundong coal in China [3]. Therefore, a better understanding is urgently required of the fundamental mechanisms driving the formation and transformation of alkali species and their interactions with complex multi-phase turbulent reacting flows during coal and biomass combustion.

Over the past few decades, experimental research on sodium release and reacting dynamics evolves from offline to online measuring techniques using advanced laser diagnostics, e.g., [4–6]. On the numerical side, a one-step Arrhenius model has been firstly proposed by van Eyk et al. [7] for sodium release during the combustion of a single char pellet. In recent works [5,6], a two-step kinetics model, which is able to describe sodium release in all stages of coal combustion, has been developed based on the simultaneous measurements of the sodium release, surface temperature and diameter of a burning coal pellet. These sodium release models are suitable to be applied in circulating fluidized bed (CFB) combustion, since the coal pellet size and burnout time employed are of the order of magnitude of those of a typical CFB boiler [6]. However, the sodium release model of pulverized-coal combustion (PCC) must still be developed.

Considering the homogeneous reactions of sodium species, well-established chemical reaction mechanisms [8] are available to model the final forms of alkali species in post-combustion gases. To the best of our knowledge, however, the dynamic of sodium release and the reaction characteristics in turbulent pulverized-coal combustion have not been investigated yet. Flow-resolved or quasi-direct numerical simulation of pulverized-coal combustion (PCC-DNS) has been attempted recently [9,10], as the sharply increasing computing capacity now allows for investigating the complex multi-physics PCC phenomenon. Since the turbulence-chemistry interaction is not modeled but resolved in these simulations, the results provide precious insights into the combustion characteristics of turbulent pulverized-coal flames and also serve as reference for subgrid scale modeling development.

Since its pioneer introduction in Reynolds-Averaged Navier–Stokes (RANS) modeling of turbulent premixed flames [11], the tabulated chemistry methods, e.g., flamelet generated manifolds (FGM) [12,13], have shown great potential on predicting major hydrocarbon and also minor species, such as NO_x [14,15].

Within this context, the aim of the present study is twofold. First, the responses of sodium species in the early stage of a three-dimensional (3D) turbulent pulverized-coal flame are simulated and analyzed, with char reaction ignored. Second, the possibility of modeling the reaction dynamics of these chemical species using one-dimensional (1D) premixed FGM is examined. In a previous study [16], a tabulation method of sodium species in PCC was proposed assuming the sodium reactions to take place only once the hydrocarbon combustion has reached its equilibrium state. Here, the coupling between sodium reactions and hydrocarbon combustion is directly accounted for in the three-dimensional simulations, in which the flow and the flame are fully resolved. The coal particles are modelled as Lagrangian point sources, with a two-way coupling with the flow (mass, momentum and energy). In the vast literature on multi-phase flow, these simulations are sometimes called 'quasi-DNS' or 'point-particle DNS'. To ease the reading, our simulation will be denoted 'DNS' in the following, still keeping in mind that the internal structure and the boundary layers of the coal particles are not resolved.

2. Pulverized-coal flame configuration and numerics

A three-dimensional temporally evolving planar pulverized-coal jet flame is studied (Fig. 1). The physical dimensions of the computational domain composed of 8.38 M cells are $L_x = 25.6$ mm, $L_y = 25.6$ mm and $L_z = 12.8$ mm. A uniform mesh of $h = 100$ μm is employed and the time step is 4.8 μs (CFL < 0.8) with sub-iteration in a stiff chemistry dedicated solver, which is further discussed below (Section 2.4) in terms of flame resolution. Initially, high-speed primary air (bulk velocity: 15 m/s, 300 K) ladened with coal particles is introduced for $|y| < 2.5$ mm. This flow is surrounded by a low-speed hot coflow of burnt gases (3 m/s, 1559 K). The locations of the coal particles follow a random uniform distribution, with a particle density of 1400 kg/m^3. The initial number of particles is 21,945 with a mono-disperse distribution of diameter of 25 μm. The coal properties are those of the Loy Yang brown coal, for which coal analysis data can be found in [16,17]. The percentage of sodium that is releasable during the coal pyrolysis stage is set to 19.1%, according to [17]. The coflowing stream carries the burnout products of the same coal volatiles at an equivalence ratio of 0.45. This stream promotes the ignition of the coal particles, as mixing with burnt products would do in a real burner. Periodic boundary conditions are employed in all directions. Turbulent fluctuations of 1.2 m/s (8% of the primary air velocity) are initially added within the shear layers between the air jet and the coflow, to facilitate the flow destabilisation. The parameters of the present PCC case, e.g., the coflow temperature and mass loading ratio of coal particles, are chosen according to jet flame

Please cite this article as: K. Wan et al., Alkali metal emissions in early stage of a pulverized-coal flame: DNS analysis of reacting layers and chemistry tabulation, Proceedings of the Combustion Institute (2018), https://doi.org/10.1016/j.proci.2018.06.119

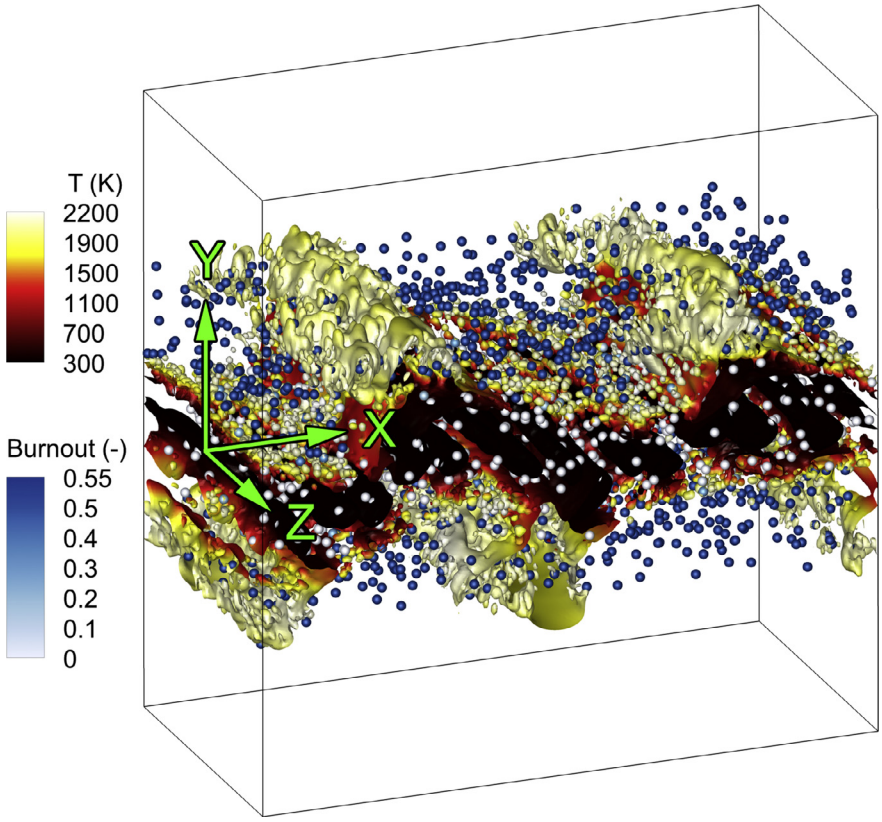

Fig. 1. Instantaneous pulverized-coal particle distribution and iso-Q criterion [19], $Q = 10^5$ s^{-2}, colored by gas temperature. The coal particles are colored by the burnout, which denotes the ratio of the released volatile mass to the initial mass of volatile in a pulverized-coal particle.

studies [16,18], with adjustments to ease DNS but without change to the multiphase reacting flow dynamics.

Coal pyrolysis, including sodium release, gas phase volatile combustion and sodium reactions are simulated. Heterogeneous char reaction is not considered here, because the contribution of char reaction should be weak in such a small-scale PCC flame, as already discussed in [13,16,20]. In addition, char reaction is much slower than homogeneous gas phase combustion and, under the present conditions, sodium reactions are found to be completed within these shorter time scales.

Figure 1 shows an instantaneous snapshot of the planar pulverized-coal flame. The turbulent flow structures are visualized via the iso-surface of Q criterion (second invariant of the velocity gradient tensor) [19] $= 10^5$ s^{-2} and colored by gas temperature. The instantaneous distribution and burnout of each particle are also illustrated.

2.1. Gas phase and pulverized-coal particles

The governing equations for the gas phase and the pulverized-coal particles are solved in the Eulerian and Lagrangian frameworks, respectively, with a low-Mach number in-house code specialised in the simulation of turbulent coal flames [16,18,21]. The conservation equations for mass, momentum, species and temperature of the gas phase are those of Wan et al. [18], in the present study without the subgrid scale modeling terms. The Lewis number (Le = 1.0) and the Prandtl number (Pr = 0.7) are assumed to be constant.

The momentum and the temperature equations of the Lagrangian coal particles are also those of Wan et al. [18]. Radiative heat transfer is solved with the Discrete Ordinates Method (DOM) [22]. The particle emissivity ε_p is set to 0.9 [23]. The gas absorption coefficient is determined by the weighted-sum-of-the-gray-gases model (WSGGM) [24]. Finally, the mass loss rate of each coal particle ($\mathrm{d}m_p/\mathrm{d}t$), due to the pyrolysis, is predicted by the single first-order reaction model (SFOM) proposed by Badzioch and Hawskley [25]. The kinetic parameters of the SFOM model, i.e., A_v (9×10^5 s^{-1}), E_v (6×10^4 J/mol) and Q_v (1.05), have been calibrated by the chemical percolation devolatilization (CPD) model, as in [21].

Please cite this article as: K. Wan et al., Alkali metal emissions in early stage of a pulverized-coal flame: DNS analysis of reacting layers and chemistry tabulation, Proceedings of the Combustion Institute (2018), https://doi.org/10.1016/j.proci.2018.06.119

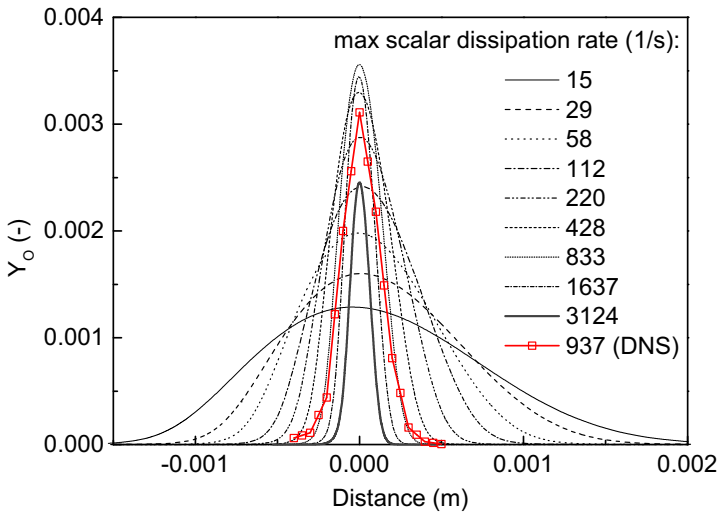

Fig. 2. Comparison of O radical profiles between DNS results and 1D counterflow diffusion flames at various strain rates. The maximum scalar dissipation rate of each profile is denoted.

2.2. Gas phase chemistry

The volatiles react according to the previously validated DRM22 skeletal mechanism by Kazakov and Frenklach [26], involving 104 elementary reactions and 22 chemical species. The compositions/mass fractions of the volatile fuels, including CH_4/0.037, C_2H_2/0.309, CO/0.208, CO_2/0.155, H_2/0.030, H_2O/0.261, are obtained from the CPD model [18,21]. The Tar species is replaced by C_2H_2 [20]. The compositions predicted by the CPD model are slightly adjusted to fulfil the elemental mass conservation.

The detailed reaction mechanism of alkali metal species by Glarborg and Marshall [8] includes 105 elementary reactions over the elements Na, K, C, H, O, S and Cl. In the present study, only the subset with the elements Na, C, H, and O is considered, which includes five sodium species, i.e., Na, NaO, NaO_2, NaOH and $Na_2O_2H_2$, and 24 elementary reactions. Considering that the sodium vapor generated inside the porous structure of a coal particle will be transported outward by the volatile yielded during the pyrolysis stage and that the sodium release was found proportional to the burnout of a coal particle during the early combustion stage [6], the sodium release rate is assumed to be proportional to the volatile release rate [16]. As in our previous study [16], atomic sodium is the alkali species released from coal in the simulation.

2.3. Numerical schemes

The numerics is based on an approach previously used for both DNS and large eddy simulation (LES) [27,28]. The time advancement uses a second-order Crank–Nicolson scheme. A Quadratic Upstream Interpolation for Convective Kinematics (QUICK) scheme is used for the scalar advection terms in the species and temperature equations, while a second-order central difference scheme is applied to the scalar diffusion terms in the species and temperature equations and all terms in the momentum equation. An Alternating Direction Implicit (ADI) method has been employed, in which semi-implicit tridiagonal/pentadiagonal equations are solved separately for each direction. The particle equations are explicitly advanced using a second-order Runge–Kutta (RK2) scheme.

2.4. Verification of the grid resolution

Before proceeding with the analysis, the resolution level of the scalar signals within the reaction zones is analyzed. Figure 2 shows the comparison of O radical profiles from the DNS and from one-dimensional counterflow diffusion flames computed for various strain rates with CANTERA [29], for the present volatile fuel and oxidizer conditions. The DNS profile is extracted from the location where the mixture fraction scalar dissipation rate, χ_Z, reaches its maximum, which matches here the maximum burning rate. According to non-premixed flame theory, the thinner reaction zones should be found for such intense burning rates and high level of χ_Z [30]. It can be observed in Fig. 2 that the reaction zone is well resolved, as there are more than 10 grid points inside this thinner flame layer. In addition, the maximum scalar dissipation rate in the DNS ($\chi_Z = 937\ s^{-1}$) is found well below the quenching point ($\chi_Z = 3124\ s^{-1}$). Interestingly, the Y_O DNS signal also fits within the expected ranges observed in the diffusion flamelet computations. A similar analysis

Please cite this article as: K. Wan et al., Alkali metal emissions in early stage of a pulverized-coal flame: DNS analysis of reacting layers and chemistry tabulation, Proceedings of the Combustion Institute (2018), https://doi.org/10.1016/j.proci.2018.06.119

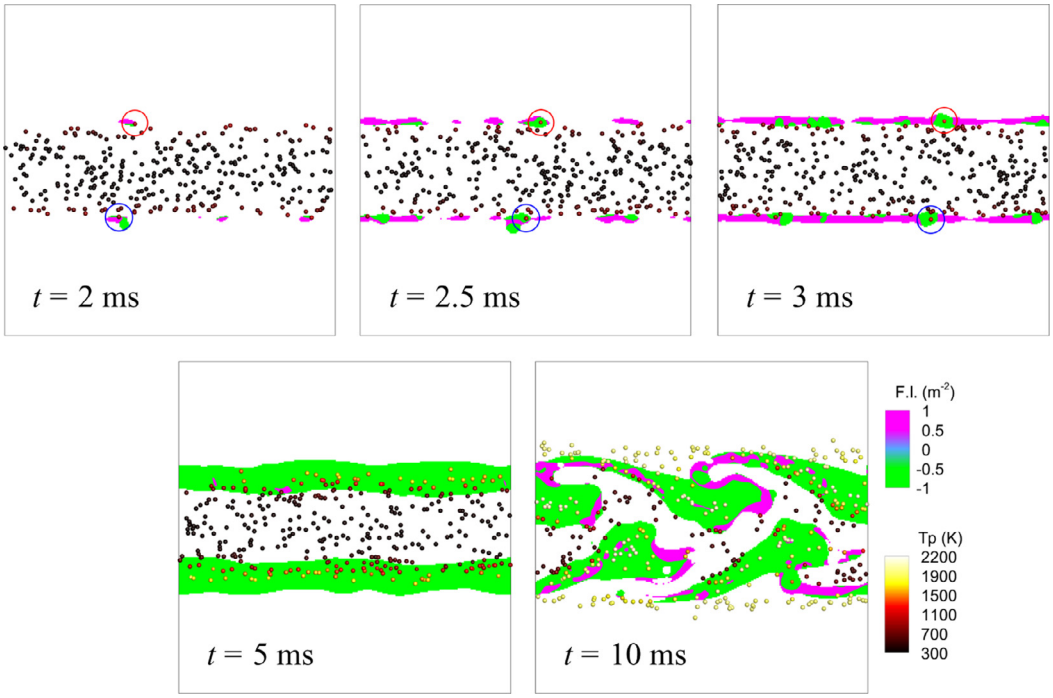

Fig. 3. Instantaneous distributions of flame index at the plane $z = 0$, at locations, where heat release rate exceeds 10^7 W/m^3. Coal particles in the region of $|z| \leq 100$ μm are shown and colored by particle temperature.

has been carried out with the partially premixed flames introduced thereafter for chemistry tabulation. The preheating of the reactants combined with the overall low levels of equivalence ratios due to the pyrolyzed character of the fuel make the flame thick, and a similar conclusion is reached concerning the required resolution.

3. Analysis of flame and sodium emission dynamics

3.1. Flame regimes

The combustion characteristics of the pulverized-coal flame are studied using the flame index, F.I. [9,31]. It is calculated from the spatial gradients of the mass fractions of the volatile fuel and the oxidizer as: F.I. $= \nabla Y_f \cdot \nabla Y_{O_2}$, where $Y_f = Y_{CH_4} + Y_{CO} + Y_{C_2H_2} + Y_{H_2}$. Positive values of F.I. are likely to indicate premixed flame regimes, while negative ones probe diffusion flame regimes. Figure 3 shows the instantaneous distributions (plane of $z = 0$) of F.I. in the regions where the heat release rate exceeds 10^7 W/m^3 and therefore where the combustion actively happens. The maximum heat release rate in the 3D domain is 2.37×10^{10} W/m^3.

First, the coal particles in the shear layers are heated up by the high-temperature coflow. Pyrolysis takes place and the volatile starts to escape from the particles to mix with the surrounding air. The first ignition is thus controlled by homogeneous combustion, with spots dominated by premixed regimes ($t \leq 3$ ms). However, in the region around particles with the highest temperatures, the diffusive combustion mode also appears because of higher fluxes of volatile release, which allow for the fuel to accumulate before burning against air ($t = 2.5$ and 3 ms). Later on, more and more particles take part in pyrolysis due to turbulent mixing and the volatile mass fraction further increases, leading to a dominant diffusion combustion mode ($t = 5$ and 10 ms). A global observation that is now refined from a direct analysis of the scalar fields.

3.2. Sodium species dynamics

Figure 4 shows the scatter plots of instantaneous mass fractions of the five sodium species against the mixture fraction, Z, at $t = 5$ ms. The mixture fraction is defined as $Z = 1.0 - Y_{N_2}/0.767$ ($Z = 1$ in the pure volatile fuel, $Z = 0$ in the oxidizer and $Z = 0.068$ in the coflow). The data is obtained from the entire 3D domain. In agreement with our previous study [16], Na and NaOH are the two major sodium species. Y_{Na} stays almost zero for $Z < 0.05$, to then increase almost linearly with the mixture fraction. Y_{NaOH} features a more subtle distribution. A first peak is reached around $Z = 0.05$, to drop to a much lower value under the

Please cite this article as: K. Wan et al., Alkali metal emissions in early stage of a pulverized-coal flame: DNS analysis of reacting layers and chemistry tabulation, Proceedings of the Combustion Institute (2018), https://doi.org/10.1016/j.proci.2018.06.119

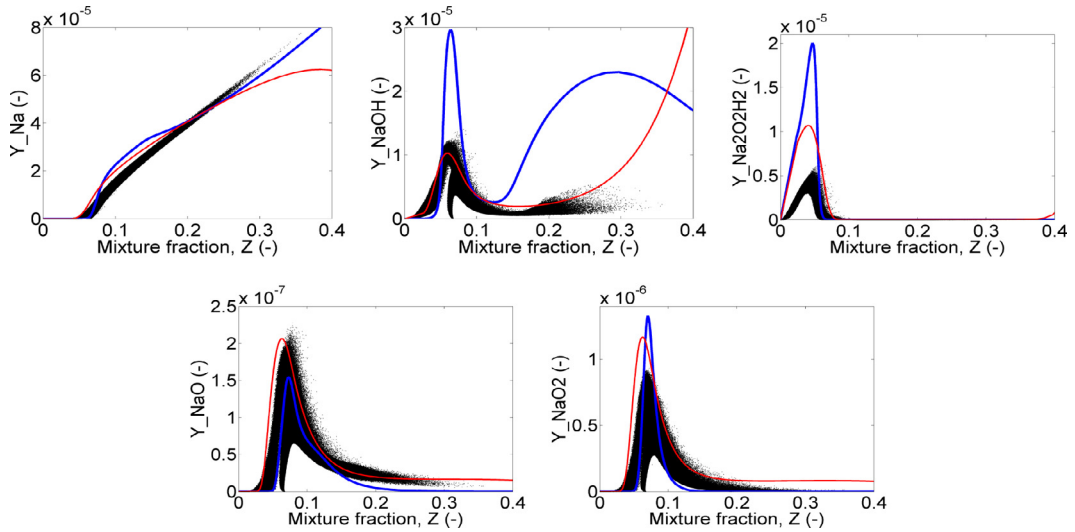

Fig. 4. Scatter plots of instantaneous mass fractions of the five sodium species against Z at $t = 5$ ms. Blue thick line and red thin line are the sodium profiles obtained from 1D counterflow diffusion flames, corresponding to the lowest (37 s^{-1}) and highest strain rates (5246 s^{-1}). (For interpretation of the references to color in this figure legend, the reader is referred to the web version of this article.)

stoichiometric condition ($Z_{st} = 0.138$), to increase again for higher equivalence ratios. The sharp decrease of Y_{NaOH} around $Z = 0.068$ results from the coflow of burnt gases, which does not carry sodium species. Finally, $Y_{Na_2O_2H_2}$ also features a relatively high concentration in the fuel-lean regime ($Z < 0.138$); while Y_{NaO} and Y_{NaO_2} remain at lower concentrations over the mixing layers.

Interestingly, the sodium chemistry response differs from the one of usual hydrocarbon diffusion flames. For instance at high-strain rate (red line) in the 1D counterflow flame, fast mixing promotes low temperature sodium reactions, with the production of NaOH on the rich side and a decrease of Na concentration at $Z = 0.4$ (Fig. 4). Compared with the sodium profiles obtained from 1D counterflow diffusion flames, many points of the turbulent flame fall outside the region between the profiles corresponding to the lowest and highest strain rates (Fig. 4). Because the maximum scalar dissipation rate in the DNS stays below the quenching limit of steady flamelets (Fig. 2), these points are likely to be representative of unsteadiness and/or partial premixing of the reactants. Accordingly, the tabulation of sodium species will now be attempted using premixed flamelets rather than steady diffusion flamelets. Indeed, the fresh mixture gets partially premixed quite rapidly after being ejected from the particles and the gradients of thermochemical quantities across iso-equivalence ratio surfaces stay moderate compared to gradient in other directions (as also previously reported in the literature at many places for for fuels released from a disperse phase, see for instance [32].)

4. Premixed flamelet generated manifold for sodium

4.1. Lookup table construction

The FGM approach was first applied in pulverized-coal combustion by Knappstein et al. [13] recently. Here it is used to tabulate the sodium chemistry. A set of one-dimensional freely propagating and laminar premixed flames are computed with CANTERA [29], as in the DNS with the DRM22 mechanism [26] for the combustion of volatiles and the detailed sodium reaction mechanism [8]. Volatile species including atomic sodium are mixed with air at various equivalence ratios. The reaction progress variable is defined as $Y_c = Y_{H_2O} + Y_{CO} + Y_{CO_2}$. To build the lookup table, the flamelet computation is repeated over a range of equivalence ratios, mapped in the mixture fraction Z, and also varying total enthalpy levels, with the Lewis number chosen at unity for all the species. The responses in the physical space are then remapped ($x = x(Y_c)$) into the progress variable space ($Y_i(x) = Y_i(Y_c)$), for every mixture fraction and total enthalpy levels (H), leading to $Y_i = Y_i(Z, Y_c, H)$. The progress variable Y_c is normalized by its bounds versus equivalence ratio before being stored in the table, to define a normalized progress variable C (Y_c is solved with the flow not C). When Z is outside the flammability limits, linear interpolations between chemical equilibrium and the mixing line are performed, to obtain the required information during the construction of the table. Hence, the final lookup table

Please cite this article as: K. Wan et al., Alkali metal emissions in early stage of a pulverized-coal flame: DNS analysis of reacting layers and chemistry tabulation, Proceedings of the Combustion Institute (2018), https://doi.org/10.1016/j.proci.2018.06.119

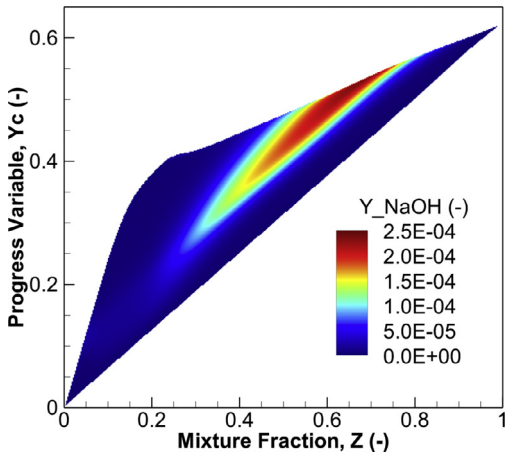

Fig. 5. FGM lookup table of Y_{NaOH} *vs* mixture fraction and progress of reaction. Baseline enthalpy level, i.e., no heat loss.

is parameterized by three coordinates: the mixture fraction, the total enthalpy and the progress variable. The manifold is mapped on to 101 × 8 × 101 data points for $Z \times H \times C$. Figure 5 shows the responses of a major sodium species, Y_{NaOH}, to Z and Y_c. To verify the lookup table discretization and the multi-linear interpolations, as in [16], one-dimensional premixed flames were first solved with the progress variable and the lookup table, selecting conditions between tabulated ones, and the results compared with success against the detailed chemistry solution.

4.2. Comparison against DNS

The reference three-dimensional DNS including the two kinetics (the DRM22 mechanism for hydrocarbon and the transported Na species) is complemented by a simulation in which the DRM22 is kept, but the FGM lookup table replaces the transport by the flow of the Na species. The thermal effect induced by the coflowing stream of burnt gases is accounted for through the tabulation versus total enthalpy, while the dilution of Na by those inert burnt gases is calibrated with an additional passive scalar.

The results closely follow those of the DNS for both major and minor sodium species (Fig. 6). The hydrocarbon species are almost unchanged, because of the very small concentrations of Na species, which do not affect much the hydrocarbon kinetics (not shown for brevity).

Figure 7 shows the scatter plots of instantaneous mass fractions of the five sodium species predicted by the FGM tabulation against those by

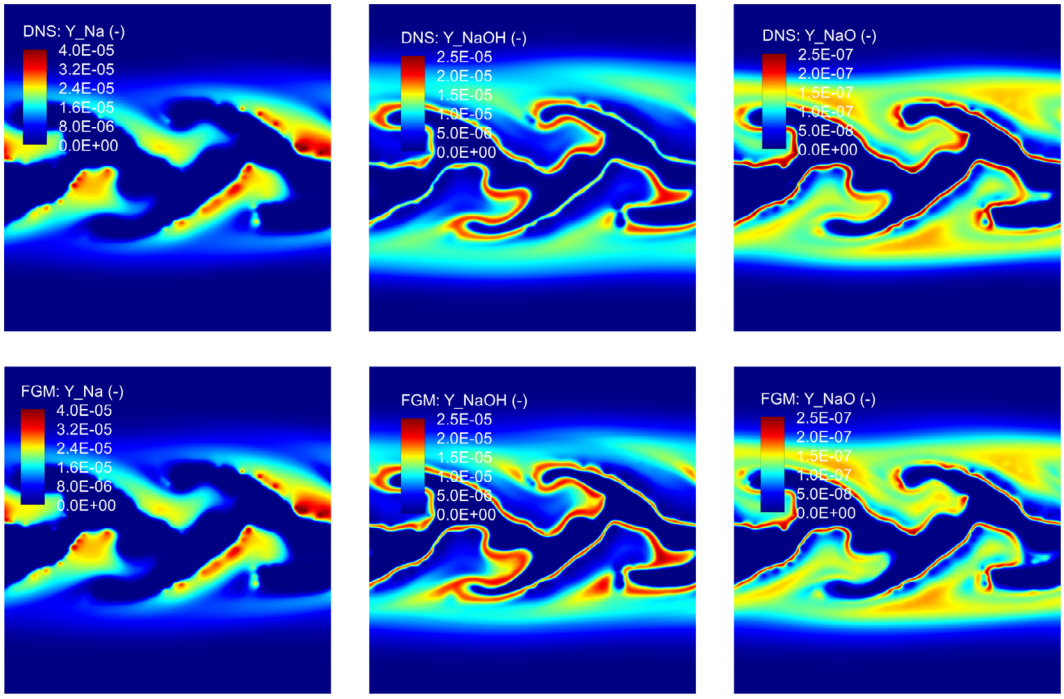

Fig. 6. Comparison of Na, NaOH and NaO predicted by the DNS (top) and the FGM (bottom) sodium tabulation approach at $t = 10$ ms.

Please cite this article as: K. Wan et al., Alkali metal emissions in early stage of a pulverized-coal flame: DNS analysis of reacting layers and chemistry tabulation, Proceedings of the Combustion Institute (2018), https://doi.org/10.1016/j.proci.2018.06.119

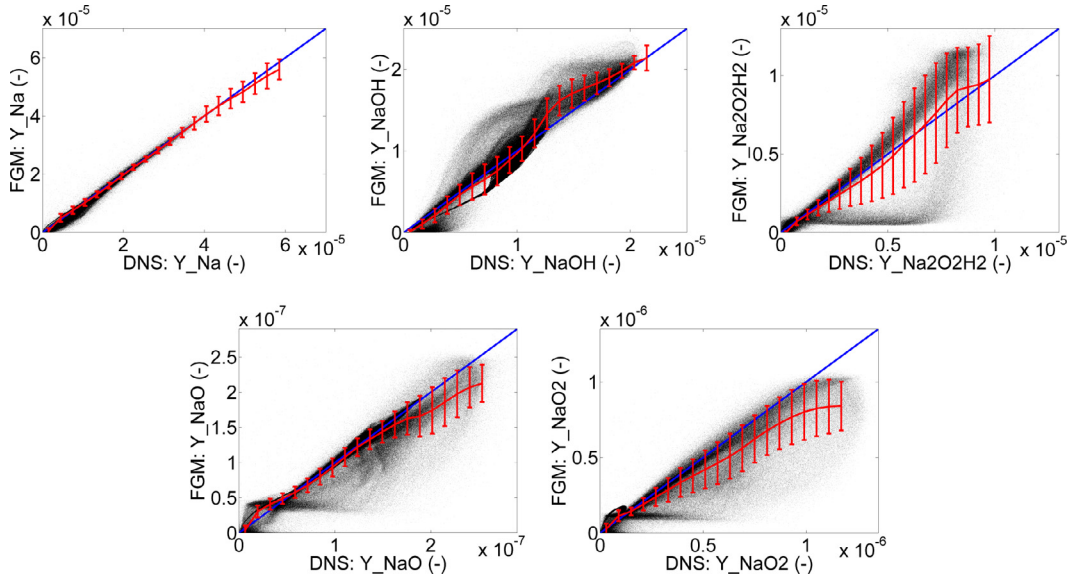

Fig. 7. Scatter plots of instantaneous mass fractions of the five sodium species predicted by the FGM tabulation method against those by DNS at $t = 10$ ms. Red line: conditional mean and fluctuation of the FGM predictions. Blue line: Perfect correlation. (For interpretation of the references to color in this figure legend, the reader is referred to the web version of this article.)

Table 1
Pearson correlation coefficients of the five sodium species predicted by the DNS and the FGM sodium chemistry table at different time instants.

Time	Na	NaOH	$Na_2O_2H_2$	NaO	NaO_2
3 ms	0.989	0.973	0.947	0.963	0.969
5 ms	0.999	0.979	0.912	0.977	0.969
10 ms	0.997	0.971	0.923	0.981	0.948

DNS at $t = 10$ ms. For the two major sodium species, i.e., Y_{Na} and Y_{NaOH}, the conditional means of the FGM predictions agree well with the DNS results. Among the other minor sodium species, the FGM conditional means of $Y_{Na_2O_2H_2}$ match the DNS results well with a slightly large uncertainty. For Y_{NaO} and Y_{NaO_2}, the FGM conditional means and DNS results agree well, except that the FGM tends to slightly under predict them under a high concentration of Y_{NaO} and Y_{NaO_2}. It can be found that accurate prediction of minor sodium species with FGM is more difficult, since the mass fractions of minor sodium species are much lower and they are more sensitive to the temperature and compositions of the gas phase. To better quantify the performance of the lookup table, the Pearson correlation coefficient ($r \in [0, 1]$) [33] is computed for the predictions of the five sodium species in DNS and FGM. As shown in Table 1, $r > 0.9$ is achieved for all the sodium species at various time instants, considering the grid points where $Y_{sodium} > 0$ of the entire domain, thus confirming the potential of the proposed strategy.

5. Summary

A temporally evolving planar pulverized-coal jet flame is simulated with complex chemistry, to account for both the combustion of volatile hydrocarbons [26] and the reactions of sodium species [8], which are released from the burning coal particles. From the flame index, combustion is found to start preferentially in partially premixed flames during the ignition stage, to then evolve toward diffusion-like reactive layers where the diffusive combustion mode dominates, with however partial premixing of the reactants. Among the five sodium species, Na and NaOH are found to be the two major ones. Y_{Na} increases along with the mixture fraction Z; while Y_{NaOH} feature a complex behaviour, as it reaches higher values at both fuel-lean and fuel-rich sides, to drop to a much lower level under the stoichiometric condition.

A sodium chemistry lookup table is constructed from laminar one-dimensional premixed flames at various mixture fractions and enthalpy levels, thus following an FGM tabulation strategy. Three-dimensional simulations are performed with the lookup table for sodium species, keeping the remaining parts of the modeling unchanged. Both major and minor sodium species predicted by FGM tabulation method closely follows the

Please cite this article as: K. Wan et al., Alkali metal emissions in early stage of a pulverized-coal flame: DNS analysis of reacting layers and chemistry tabulation, Proceedings of the Combustion Institute (2018), https://doi.org/10.1016/j.proci.2018.06.119

reference simulation, with a Pearson correlation coefficient larger than 0.9.

Acknowledgments

This work was jointly supported by the National Natural Science Foundation of China (51706200, 51390491, 51422605), the China Postdoctoral Science Foundation (2018M632460), the Royal Society and the Engineering and Physical Sciences Research Council (EPSRC) of the UK. Special thanks are due to Prof. Peter Glarborg of DTU, who provided us the detailed mechanism of alkali metal species. Computing resources were provided by CRIANN (http://www.criann.fr).

References

[1] IEA, Key world energy statistics, 2017.
[2] Y. Niu, H. Tan, S. Hui, *Prog. Energy Combust. Sci.* 52 (2016) 1–61.
[3] G. Song, X. Qi, W. Song, Q. Lu, *Energy Fuels* 30 (5) (2016) 3967–3974.
[4] Y. He, J.J. Zhu, B. Li, et al., *Energy Fuels* 27 (2) (2013) 1123–1130.
[5] Z.H. Wang, Y.Z. Liu, R. Whiddon, et al., *Combust. Flame* 176 (2017) 429–438.
[6] Y.Z. Liu, Y. He, Z.H. Wang, et al., *Combust. Flame* 189 (2018) 77–86.
[7] P.J. van Eyk, P.J. Ashman, G.J. Nathan, *Combust. Flame* 158 (12) (2011) 2512–2523.
[8] P. Glarborg, P. Marshall, *Combust. Flame* 141 (12) (2005) 22–39.
[9] T. Hara, M. Muto, T. Kitano, R. Kurose, S. Komori, *Combust. Flame* 162 (12) (2015) 4391–4407.
[10] M. Muto, K. Yuasa, R. Kurose, *Fuel* 190 (2017) 136–144.
[11] D. Bradley, L. Kwa, A. Lau, M. Missaghi, S. Chin, *Combust. Flame* 71 (2) (1988) 109–122.
[12] J.A. van Oijen, F.A. Lammers, L.P.H. de Goey, *Combust. Flame* 127 (3) (2001) 2124–2134.
[13] R. Knappstein, G. Kuenne, A. Ketelheun, et al., *Combust. Flame* 169 (2016) 72–84.
[14] G. Godel, P. Domingo, L. Vervisch, *Proc. Combust. Inst.* 32 (2009) 1555–1561.
[15] F. Pecquery, V. Moureau, G. Lartigue, L. Vervisch, A. Roux, *Combust. Flame* 161 (2) (2014) 496–509.
[16] K.D. Wan, J. Xia, L. Vervisch, Y.Z. Liu, Z.H. Wang, K.F. Cen, *Combust. Theory Model.* 22 (2) (2018) 203–236.
[17] P.J. van Eyk, P.J. Ashman, Z.T. Alwahabi, G.J. Nathan, *Combust. Flame* 158 (6) (2011) 1181–1192.
[18] K.D. Wan, J. Xia, Z.H. Wang, M. Pourkashanian, K.F. Cen, *Flow Turbul. Combust.* 99 (2) (2017) 531–550.
[19] J.C.R. Hunt, A.A. Wray, P. Moin, *Center for Turbulence Research Proceedings of the Summer Program* CTR-S88 (1988) 193–208.
[20] M. Rieth, A. Clements, M. Rabaçal, F. Proch, O. Stein, A. Kempf, *Proc. Combust. Inst.* 36 (2) (2017) 2181–2189.
[21] K.D. Wan, J. Xia, Z.H. Wang, L.C. Wrobel, K.F. Cen, *Combust. Sci. Technol.* 189 (1) (2017) 103–131.
[22] S. Chandrasekhar, *Radiative Transfer*, Dover Publications, New York, 1960.
[23] K.D. Wan, Z.H. Wang, Y. He, et al., *Fuel* 139 (2015) 356–364.
[24] T.F. Smith, Z.F. Shen, J.N. Friedman, *J. Heat Transfer* 104 (4) (1982) 602–608.
[25] S. Badzioch, P.G.W. Hawksley, *Ind. Eng. Chem. Process Des. Develop.* 9 (4) (1970) 521–530.
[26] A. Kazakov, M. Frenklach, Reduced reaction sets based on GRI-Mech 1.2, 1994, (http://www.me.berkeley.edu/drm/).
[27] C. Pierce, P. Moin, *J. Fluid Mech.* 504 (2004) 73–97.
[28] O. Desjardins, G. Blanquart, G. Balarac, H. Pitsch, *J. Comput. Phys.* 227 (15) (2008) 7125–7159.
[29] D.G. Goodwin, H.K. Moffat, R.L. Speth, Cantera: an object-oriented software toolkit for chemical kinetics, thermodynamics, and transport processes, 2017, (http://www.cantera.org). Version 2.3.0. https://doi.org/10.5281/zenodo.170284.
[30] N. Peters, *Turbulent Combustion*, Cambridge University Press, Cambridge, 2000.
[31] P. Domingo, L. Vervisch, J. Réveillon, *Combust. Flame* 140 (3) (2005) 172–195.
[32] J. Reveillon, L. Vervisch, *J. Fluid Mech.* 537 (2005) 317–347.
[33] K. Pearson, *Proc. R. Soc.* 58 (1895) 240–242.

Please cite this article as: K. Wan et al., Alkali metal emissions in early stage of a pulverized-coal flame: DNS analysis of reacting layers and chemistry tabulation, Proceedings of the Combustion Institute (2018), https://doi.org/10.1016/j.proci.2018.06.119